

ORIGINAL RESEARCH ARTICLE

# Statistical analysis of wind energy potential in Mongo, Chad, for small-scale renewable applications

Ali Sidick Bahar<sup>1</sup>, Adoum Kriga<sup>1</sup>, Ali Ramadan Ali<sup>1</sup>, Abakar Mahamat Tahir<sup>2</sup>,  
Adoum Danao Adile<sup>1</sup>, and Fabien Kenmogne<sup>3\*</sup> 

<sup>1</sup>Department of Industrial Engineering and Maintenance, Faculty of Engineering Sciences and Techniques,  
Polytechnic University of Mongo, Mongo, Guéra region, Chad

<sup>2</sup>Laboratory of Renewable Energy and Materials Premises, Faculty of Exact and Applied Sciences,  
University of Ndjamen, Ndjamen, Chad

<sup>3</sup>Department of Civil Engineering, Advanced Teachers Training College of the Technical Education,  
University of Douala, Douala, Littoral Region, Cameroon

\*Corresponding author: Fabien Kenmogne (kenfabien@yahoo.fr)

*Received: February 10, 2025; 1st revised: March 17, 2025; 2nd revised: May 5, 2025; 3rd revised: July 14, 2025;  
Accepted: July 15, 2025; Published online: August 6, 2025*

**Abstract:** Wind plays a crucial role in various physical applications, including wind energy and pollutant transport and diffusion. Wind varies from both temporal and spatial perspectives. This paper presents a statistical analysis of wind energy potential in Mongo, the capital city of Guéra Province, Chad, using 11 years of data obtained from the local meteorological station. Using the Weibull distribution function, we analyzed the wind speed probability distributions based on the wind data obtained. The obtained results, based on average annual wind speed and energy generation, indicate that Mongo is suitable only for small-scale wind energy applications. The average wind speed within the chosen time interval is 3.2 m/s, which is classified as Class 1 according to the international system of wind classification. Wind rose plots illustrate that the wind directions vary across the years. The temperature data were also plotted, reporting an average temperature of 27.76°C over the 11-year study period. This indicates that Mongo has a relatively hot climate, which may contribute to the modest but consistent wind speeds observed in this city.

**Keywords:** Wind energy potential; Renewable energy; Wind and temperature data; Weibull distribution function.

## 1. Introduction

Access to electricity remains a critical challenge in Chad, a landlocked Central African country with one of the lowest electrification rates globally. As of 2021, only about 8% of the total population had access to electricity, with rural areas reporting coverage as low as 1.3%.<sup>1,2</sup> This energy poverty significantly hinders social and economic development by limiting access to

essential services, such as healthcare, education, clean water, and communication.<sup>3,4</sup> The government of Chad has initiated efforts to diversify its energy portfolio by integrating renewable energy sources, including solar and wind, into its national energy mix.<sup>5-7</sup> Given Chad's challenging energy access and the low electrification rates, especially in rural areas, such as Guéra Province, where Mongo is located, assessing Mongo's wind energy potential is crucial for identifying viable local

solutions that can foster sustainable development and improve living standards. This focus aligns with the national aims of expanding decentralized renewable energy systems to underserved regions.<sup>4,5</sup>

Wind energy, as a globally recognized clean and renewable resource, has been extensively studied to address energy access challenges. Recent scientific literature provides a comprehensive and up-to-date basis for assessing and deploying wind energy in contexts comparable to Chad.<sup>8-23</sup> These studies encompass various statistical approaches to wind resource assessment, which demonstrate the global relevance of evaluating wind energy potential in developing regions.

Despite the country's significant potential in both fossil and renewable energy sources, including solar irradiance levels exceeding 5.5 kWh/m<sup>2</sup>/day and moderate wind corridors in various regions, the application of wind energy remains underdeveloped.<sup>8-10</sup> In response to the pressing need for sustainable energy and climate resilience, the Chadian government has prioritized the development of renewable energy through national energy planning and recent regulatory reforms, such as the 2018 Renewable Energy Promotion Law.<sup>11,12</sup> Wind energy, in particular, offers a promising solution for off-grid and rural electrification, especially in areas with moderate and consistent wind patterns.<sup>13,14</sup> Studies from countries with similar climatic conditions have shown that even moderate wind regimes, when well characterized statistically, can effectively support micro-wind energy systems.<sup>15,16</sup>

Mongo, the capital of Guéra Province, is situated in a transitional climatic zone between the Sahel and Sudanese ecological regions. Although it has not been the focus of major national wind studies, its location, topography, and meteorological conditions suggest that Mongo is a potentially viable wind resource. Previous studies, such as those by Soulouknga *et al.*<sup>2</sup> and Medjo Nouadje *et al.*,<sup>24</sup> have explored wind potential in regions, including Abéché and N'Djamena, applying the Weibull distribution model to characterize wind patterns. However, these analyses often rely on short datasets or fail to evaluate wind behavior over extended periods. Similar gaps have been observed in many developing countries, where long-term wind datasets are rare and modeling is often oversimplified.<sup>25-27</sup> In particular, no dedicated long-term study has been conducted to assess Mongo's wind energy potential using statistically robust methods and decade-long data series.

This study aims to fill that gap by conducting a comprehensive analysis of Mongo's wind potential using data collected over an 11-year period (2012 – 2022).

The combination of the Weibull distribution and the maximum entropy principle (MEP) allows for a robust and complementary characterization of the wind speed distribution, where Weibull provides a widely accepted parametric model, and Maximum Entropy offers a flexible, information-theoretic approach that can capture complex wind speed behaviors that are not always well represented by standard distributions.<sup>28-30</sup>

The goal is to determine whether Mongo is suitable for small-scale wind energy systems that support rural electrification initiatives and contribute to the national renewable energy strategy. These methods have been validated in similar assessments in North and West Africa, Central Asia, and Latin America, proving effective even in low-to-moderate wind conditions.<sup>17</sup>

The research's strengths lie in its long-term dataset, robust statistical approach, and focused geographic scope, which provide detailed, actionable insights. However, there are limitations, such as the absence of economic and technical feasibility analyses, which are proposed for future work. The study contributes to the scientific field by addressing a critical data gap for Chad and demonstrating a replicable methodology for wind resource assessment in comparable developing regions.

The relevance of this study lies in its potential to inform policy decisions and guide investment in decentralized wind energy systems for rural regions in Chad. Unlike previous research, which often covers broader geographic scopes or lacks temporal depth, this work provides a detailed, localized, and data-driven analysis focused on a specific site of strategic interest. It not only contributes to the sparse academic literature on Chad's wind energy prospects but also provides actionable insights for energy planners, engineers, and stakeholders. To guide this investigation, the following research questions are posed:

- (i) What is the average annual and monthly wind speed in Mongo over the period 2012 – 2022?
- (ii) What are the dominant wind directions, and how do they vary seasonally?
- (iii) What is the estimated wind power density and its suitability for energy generation?
- (iv) Does Mongo meet the criteria for deploying small-scale wind turbines for decentralized power generation?

In response to these questions, several hypotheses are formulated:

- (i) The availability of 11 years of data allows for statistically reliable wind speed estimation using Weibull and entropy-based models

- (ii) The average wind speed in Mongo is  $\geq 3.0$  m/s, corresponding to wind power Class 1, which is suitable for limited applications
- (iii) The prevailing wind direction is predominantly south-southwest, consistent with regional climatic patterns
- (iv) The estimated wind power density is sufficient to support standalone micro-generation systems ( $<30$  W/m<sup>2</sup>).

These hypotheses were tested through descriptive statistical analysis, parameter estimation, and comparison with international wind classification standards. The study also analyzed wind power potential using both annual and monthly assessments, accounting for variability and reliability. Although this study does not include a full economic feasibility assessment, indicative metrics, such as average power output and temporal consistency, help to determine the viability of wind exploitation in the region.

In short, this research addresses a significant knowledge gap by providing the first long-term, data-driven assessment of Mongo's wind energy potential. It contributes to national efforts to expand renewable energy access in underserved areas and offers a replicable framework for similar assessments in other regions of Chad or comparable developing contexts. While focused on localized wind resource evaluation, the study acknowledges limitations, such as the absence of economic feasibility analysis, which can be addressed in future research to strengthen deployment strategies.

## 2. Materials and methods

### 2.1. Study area and data acquisition

This study focuses on Mongo, the capital of Guéra Province in central Chad, located between latitudes 12°18' and 13°18' north and longitudes 18°07' and 19°07' east. The town lies at an elevation of approximately 415 ± 5 m above sea level on alluvial deposits, covering an area of 63.5 km<sup>2</sup>. Mongo features a Sahelian climate characterized by two distinct seasons: A rainy season from April to October and a dry season from November to March.<sup>1</sup>

Meteorological data for the period 2012 – 2022 were collected from the Mongo weather station, including monthly averages of wind speed, wind direction, and ambient temperature computed from hourly measurements. The data originate from the official Mongo meteorological station, with all instruments

complying with World Meteorological Organization standards, ensuring measurement precision of ± 0.1 m/s for wind speed and ± 0.5°C for temperature. The temporal resolution of the data used in this study is monthly, derived as averages from hourly recordings. The collected data underwent rigorous quality control to detect anomalies and interpolate missing values to ensure reliability.<sup>7,23</sup>

### 2.2. Statistical modeling of wind speed using the Weibull distribution

The statistical modeling of wind speed is crucial for accurate wind energy assessment. Among the various models proposed in the literature, the two-parameter Weibull distribution remains the most widely used due to its flexibility and good fit to empirical data across many geographical regions.<sup>12,16</sup> The Weibull probability density function (PDF) is expressed in Equation I.

$$f(v) = \left(\frac{k}{c}\right) \left(\frac{v}{c}\right)^{k-1} \exp\left(-\left[\frac{v}{c}\right]^k\right), v > 0 \quad (I)$$

where  $v$  is the wind speed (m/s),  $k$  is the dimensionless shape parameter, and  $c$  is the scale parameter (m/s). The cumulative distribution function is expressed in Equation II.

$$f(v) = 1 - \exp\left(-\left[\frac{v}{c}\right]^k\right) \quad (II)$$

The Weibull distribution was chosen for this study due to its proven versatility and widespread acceptance in wind energy assessment worldwide. Compared to other distributions, such as Rayleigh, Lognormal, Gamma, or Beta, the Weibull distribution provides a better balance between model simplicity and the ability to accurately capture a wide range of wind speed frequency patterns across diverse climatic conditions.<sup>12,16</sup> Its two parameters allow flexibility in adjusting both the shape and scale of the distribution, making it suitable for representing skewed and variable wind speed data like those observed in the Sahelian climate of Mongo.

The Weibull parameters,  $k$  and  $c$ , were estimated using two complementary approaches to ensure robustness and accuracy: The method of moments and the energy pattern factor (EPF) method.

The method of moments involves calculating the shape parameter  $k$  and scale parameter  $c$  from the sample mean and standard deviation  $\sigma_v$  of the wind speed data, as shown in Equations III and IV.

$$\bar{v} = c = \frac{\bar{v}}{\Gamma\left(1 + \frac{1}{k}\right)} \quad (\text{III})$$

$$\sigma_v = c \sqrt{\left(\Gamma\left(1 + \frac{2}{k}\right) - \left[\Gamma\left(1 + \frac{1}{k}\right)\right]^2\right)} \quad (\text{IV})$$

where  $\Gamma$  denotes the gamma function. The EPF method, based on the ratio of the third moment to the cube of the first moment of the wind speed, is defined in Equation V. The shape parameter  $k$  is calculated with Equation VI, followed by parameter  $c$  derived from  $k$  and the mean wind speed.

$$EPF = \frac{\bar{v}^3}{\bar{v}^3} = \frac{\frac{1}{n} \left(\sum_{i=1}^n v_i^3\right)}{\left(\frac{1}{n} \sum_{i=1}^n v_i\right)^3} \quad (\text{V})$$

$$k = 1 + \frac{3.69}{(EPF)^2} \quad (\text{VI})$$

By applying both methods, the parameter estimates were cross-validated to ensure consistency and to improve the fit of the Weibull model to the observed wind speed data. Beyond the Weibull distribution, several other statistical models have been proposed for calculating wind speed distributions, each with its specific advantages and limitations. The Rayleigh distribution, a special case of Weibull with  $k = 2$ , has been used due to its simplicity, but may lack flexibility for complex wind regimes.<sup>11,19</sup> The Lognormal distribution has also been employed, especially when the Weibull does not efficiently capture skewness in data.<sup>17,24</sup> Advanced parametric models, such as the Gamma and Beta distributions, can fit wind speed data with multimodal features or specific skewness and kurtosis patterns.<sup>18,27,31</sup> However, these models typically require more data and computational effort, which may not always be feasible.

Weibull distribution is chosen in this study due to its proven robustness, simplicity, and widespread acceptance in wind energy studies, which makes it suitable for the available Mongo dataset. Nevertheless, to overcome limitations linked to parametric assumptions, complementary methods are considered.

### 2.3. Statistical modeling using the MEP

In addition to parametric methods, non-parametric approaches, such as the MEP have been applied to

wind speed modeling.<sup>14,20,32</sup> The MEP maximizes the Shannon entropy subject to constraints derived from empirical data, resulting in the least-biased probability distribution consistent with known information.

To provide a more intuitive understanding, the MEP can be viewed as a method for deriving the most unbiased probability distribution when only limited information (such as average values or moments) is known. By maximizing entropy, the approach avoids introducing unwarranted assumptions or bias beyond the constraints imposed by the data. This leads to a distribution that best represents the true uncertainty inherent in the wind speed data. The advantage of using MEP lies in its flexibility and minimal assumptions, allowing it to adapt to complex wind speed behaviors that may not be well captured by standard parametric models, such as Weibull. This makes MEP especially useful in environments where wind regimes are highly variable or poorly characterized by simple distributions. The constraints are: (i) The total probability within the defined speed interval must be equal to one, as shown in Equation VII; (ii) The M-low statistical orders for the theoretical and empirical distributions must be equal, as shown in Equation VIII. The general solution is shown in Equation IX.

$$\int_0^{\max(v)} f(v) dv = 1 \quad (\text{VII})$$

$$\int_0^{\max(v)} v f(v) dv = \bar{v} \quad (\text{VIII})$$

$$f(v) = \exp\left(\sum_{i=1}^M \alpha_i v^i\right) \quad (\text{IX})$$

where  $\alpha_i$  is the Lagrangian multiplier found using the Newton-Raphson method. Other non-parametric methods, including kernel density estimation and empirical distribution functions, have also been used to model wind speed without assuming a predefined functional form. These data-driven approaches can capture complex distribution shapes, but they might require large datasets to achieve their effectiveness.<sup>13,27,33,34</sup> The combined use of Weibull distribution and MEP in this study leverages the robustness and simplicity of a classical parametric model with the flexibility of a non-parametric approach, providing a comprehensive characterization of the wind speed regime at Mongo.

#### 2.3.1. Wind power density estimation

The wind power density represents the kinetic energy flux per unit area, as shown in Equation X.

$$E = \frac{P}{A} = \frac{1}{2} \rho \int_0^{\infty} v^3 f(v) dv \quad (X)$$

where  $E$  is the power density ( $\text{W/m}^2$ ),  $\rho$  is the air density ( $1.225 \text{ kg/m}^3$ ), and  $f(v)$  is the wind speed PDF (Weibull or MEP). Accurate modeling of the wind speed distribution is crucial for realistic energy yield estimates.<sup>35</sup>

### 2.3.2. Wind direction analysis using a wind rose

An assessment of wind direction was performed using monthly averaged data collected from 2012 to 2022. The directional values were categorized into 16 equally spaced compass sectors, each covering  $22.5^\circ$ , to ensure adequate angular resolution over the full  $360^\circ$  range. This segmentation enables the systematic quantification of the directional distribution of the wind over the study period.

The frequency of wind blowing from each sector is calculated with Equation XI.

$$f_i = \frac{n_i}{N} \times 100 \quad (XI)$$

where  $f_i$  is the frequency (in percent) of wind coming from direction sector  $i$ ;  $n_i$  is the number of wind direction observations in that sector, and  $N$  is the total number of valid wind direction records.

The data were processed using meteorological statistical tools capable of handling directional classification and frequency analysis. No filtering based on wind speed threshold was applied in this computation phase to preserve the full angular distribution of wind occurrence. The results of this procedure served as input for constructing a wind rose diagram, which reflects the statistical dispersion of wind direction at the site.<sup>8,36</sup>

## 2.4. Temperature analysis and wind temperature relationship assessment

Air temperature affects atmospheric pressure gradients and convective flows, shaping wind dynamics.<sup>28,29</sup> Monthly average temperatures from 2012 to 2022 were analyzed through:

- (i) Time series analysis to identify seasonal and interannual variability
- (ii) Graphical superimposition of temperature and wind speed for concurrent trend detection
- (iii) Scatter plots to assess preliminary correlations
- (iv) Regression modeling (linear and non-linear) to quantify relationships, evaluated by determination coefficient ( $R^2$ )

- (v) Hysteresis analysis to detect phase lag or cyclical wind–temperature interactions.<sup>30,37</sup>

This methodology aims to elucidate the role of temperature as a modulator of wind patterns in Mongo’s Sahelian climate, supporting refined assessments of wind energy potential.

## 3. Results and discussion

### 3.1. Wind speed analyses

Table 1 summarizes the monthly and annual mean wind speeds over the 2012 – 2022 period. All annual mean values exceed the minimum exploitable wind speed threshold of 2.0 m/s, demonstrating that Mongo has a usable, albeit modest, wind resource. The highest annual average wind speed was recorded in 2012, with 4.61 m/s, and the lowest in 2022, at 1.80 m/s. This range aligns with wind regimes classified as Class 1 under International Electrotechnical Commission standards, generally suited for small-scale or hybrid wind power applications.<sup>6,17,23,28</sup>

Figure 1 illustrates the monthly wind speed evolution over 11 years, presenting a 3D temporal profile (Figure 1A) and a 2D projection (Figure 1B). The temporal signal (Figure 2A) illustrates bursting behavior characterized by short-term spikes in wind speed, which may be attributed to local convective phenomena and regional climate influences.<sup>6,14,18</sup> The long-term monthly mean (Figure 2B) reveals a seasonal pattern with higher wind speeds during specific months, consistent with similar patterns observed in semi-arid regions, such as Central Iran and Northern India.<sup>18,19</sup> These temporal and seasonal variations underscore the importance of temporal resolution in wind resource assessment and planning. The relatively low but stable wind speeds suggest Mongo’s wind energy applications should focus on micro or small wind turbine systems designed for low-wind regimes.<sup>17,23,28</sup>

### 3.2. Probability distribution and wind power

The Weibull distribution parameters, shape factor ( $k$ ) and scale factor ( $c$ ), were computed numerically (Equations I – IV) and are presented in Table 2 for annual data, and Table 3 for monthly data. These parameters were used to construct the wind speed PDF shown in Figure 3, where the mode centers around 3.25 m/s, close to the mean wind speed. This confirms the adequacy of the Weibull model for this dataset, as supported by studies in Turkey, Iran, and Canada.<sup>12,13,15,18,23</sup>

**Table 1. Monthly and annual mean wind speeds (m/s) in Mongo from 2012 to 2022**

Month	2012	2013	2014	2015	2016	2017	2018	2019	2020	2021	2022	Mean
Jan	3.98	3.73	3.73	4.33	4.08	3.72	4.2	3.72	4.37	4.28	4.44	4.05
Feb	4.34	4.34	4.39	4.18	4.23	4.39	3.77	4.09	4.58	4.45	4.38	4.29
Mar	4.61	3.64	3.82	4.12	4.17	4.09	3.48	4.20	4.29	4.21	4.28	4.08
Apr	4.11	3.93	3.08	4.34	3.35	3.67	3.36	3.47	3.38	3.94	3.29	3.63
May	3.53	3.27	3.60	3.41	3.44	3.74	3.67	3.47	2.81	3.27	3.23	3.40
Jun	3.41	3.34	3.72	3.62	3.38	3.23	3.57	3.27	3.40	3.55	3.41	3.45
Jul	2.48	3.17	3.04	2.90	2.65	2.96	2.72	2.75	2.86	3.11	2.77	2.86
Aug	2.20	2.47	2.48	2.11	2.30	2.18	2.35	2.28	2.35	2.15	2.31	2.29
Sept	1.88	2.13	2.08	2.10	1.98	2.38	1.96	2.09	1.82	2.09	1.80	2.03
Oct	2.05	1.93	2.08	2.47	2.41	2.36	2.55	1.95	1.98	2.09	2.10	2.18
Nov	2.27	2.14	2.62	2.57	2.98	2.65	2.80	2.70	2.87	2.90	2.64	2.65
Dec	3.25	3.70	3.21	4.16	3.99	3.87	3.70	3.03	3.17	3.38	3.48	3.54
Mean	3.18	3.15	3.15	3.36	3.25	3.27	3.18	3.09	3.16	3.29	3.18	3.20

**Table 2. Annual Weibull distribution parameters and estimated wind power density (W/m<sup>2</sup>) from 2012 to 2022**

Parameter	2012	2013	2014	2015	2016	2017	2018	2019	2020	2021	2022	Mean
EPF	1.26	1.17	1.15	1.19	1.16	1.14	1.12	1.16	1.23	1.18	1.22	1.16
K	3.34	3.69	3.80	3.62	3.75	3.83	3.92	3.74	3.434	3.63	3.50	3.73
C	3.54	3.49	3.49	3.73	3.60	3.62	3.51	3.42	3.511	3.64	3.53	3.55
Power	18.57	16.90	17.58	16.65	15.92	17.84	16.09	15.45	18.57	18.05	17.49	17.19

Abbreviations: C: Scale factor; EPF: Energy pattern factor; K: Shape factor.

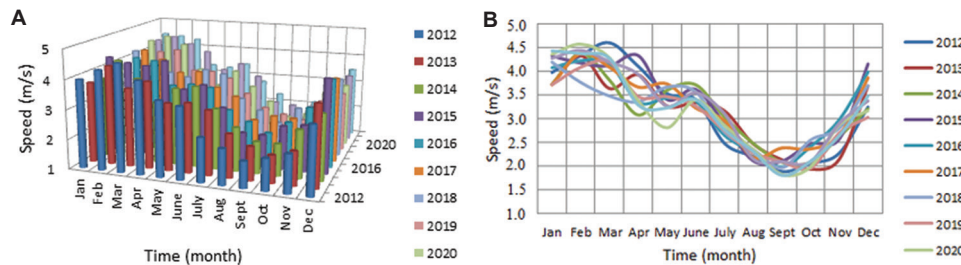


**Figure 1. Monthly wind speed profiles from 2012 to 2022. (A) 3D temporal evolution illustrating impulsive wind bursts; (B) 2D projection showing seasonal patterns.**

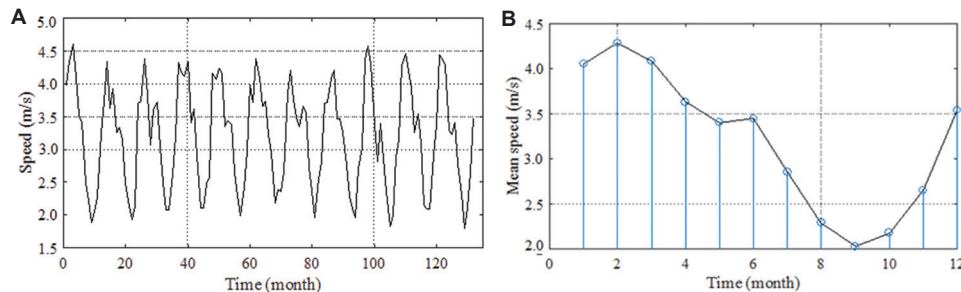


**Figure 2. Temporal evolution of wind speed in Mongo. (A) Raw monthly data from 2012 to 2022 showing burst-like variations; (B) Long-term average wind speed highlighting seasonal trends.**

**Table 3. Monthly Weibull distribution parameters and wind power density (W/m<sup>2</sup>)**

Parameter	Jan	Feb	Mar	Apr	May	Jun	Jul	Aug	Sep	Oct	Nov	Dec
EPF	1.01	1.01	1.02	1.03	1.02	1.01	1.01	1.01	1.02	1.03	1.02	1.03
K	4.59	4.64	4.57	4.46	4.58	4.65	4.59	4.63	4.56	4.48	4.51	4.47
C	4.44	4.67	4.47	3.98	3.73	3.77	3.12	2.50	2.22	2.39	2.90	3.88
Power	14.70	12.00	14.36	20.59	24.57	24.19	28.91	10.45	1.99	6.60	25.15	22.03

Abbreviations: C: Scale factor; EPF: Energy pattern factor; K: Shape factor.

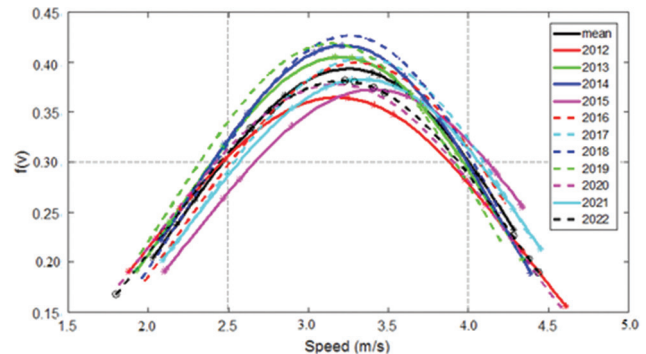
The estimated annual wind power density (Table 2) ranges from a minimum of 15.45 W/m<sup>2</sup> (2019) to a maximum of 18.57 W/m<sup>2</sup> (2012 and 2020), which classifies Mongo as a Class 1 site, suitable for small-scale wind energy projects or hybrid systems combined with solar photovoltaic.<sup>11,17,21,28,38</sup> Monthly variations (Table 3, Figure 4) indicate July as the peak month for wind power density (28.91 W/m<sup>2</sup>), and September as the lowest (1.99 W/m<sup>2</sup>), consistent with the regional climatology marked by wet and dry seasonal wind shifts.<sup>19,21,26</sup> Compared to high-potential sites (often > 100 W/m<sup>2</sup>), Mongo’s wind power density is modest but not negligible. This level is favorable for off-grid rural electrification or to supplement other renewables, especially in the context of Chad’s low electrification rates.<sup>3,4,5,30</sup>

**3.3. Wind direction analyses**

The wind rose diagrams derived from Table 4 (Figures 5 and 6) illustrate a dominant south-southwest wind direction throughout most of the years (2015 – 2022), with exceptions of northwest winds in 2013 and 2017. Seasonal analysis shows northeast and east winds predominate during dry months, while south-southwest and southwest directions dominate the wet season (June – September), a pattern consistent with the influence of Harmattan and monsoonal airflows.<sup>2,9,10,21</sup> These directional trends inform optimal turbine orientation and layout, as turbines aligned with prevailing winds achieve higher efficiency and reduced mechanical wear. The seasonal variability highlights the necessity for adaptable turbine systems or hybrid configurations to maintain steady power output year-round.<sup>31,36</sup>

**3.4. Temperature analyses**

Table 5 illustrates the monthly and annual temperature data, revealing Mongo as a hot region with mean annual temperatures ranging from 27.27°C to 28.57°C, and monthly extremes from 24.55°C to 33.19°C. These thermal conditions foster atmospheric convection, likely contributing to the impulsive wind bursts identified in the temporal wind speed data.<sup>6,14,18</sup>



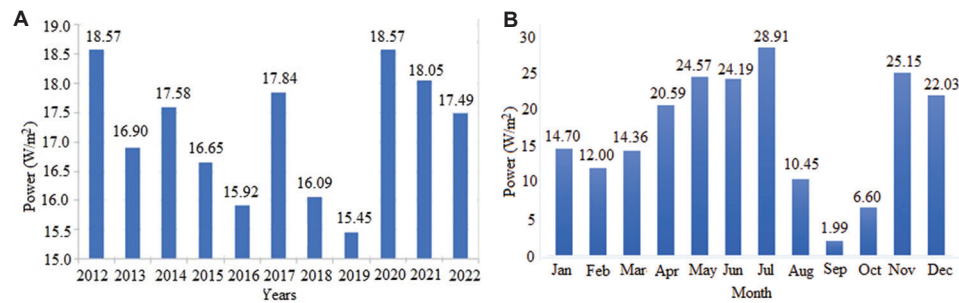
**Figure 3. Weibull probability density functions for annual wind speed in Mongo (2012 – 2022)**

Figure 7A and B show the temperature trends in 3D and 2D views, while Figure 8A and B depict the raw and mean temporal signals, both exhibiting quasi-periodic bursting signals. The dependency between temperature and wind speed demonstrates a non-linear relationship in the hysteresis form, a phenomenon arising from complex interactions involving air density changes, local pressure gradients, and boundary layer dynamics.<sup>14,20,24,37,39-41</sup> Other influences, such as topographical features, humidity, and diurnal solar heating cycles, may affect this non-linear dependency, highlighting the need for finer temporal and spatial resolution data, as well as more advanced modeling to accurately characterize wind-temperature dynamics in Mongo.<sup>32,37</sup>

**3.5. Environmental and sustainability implications**

The results show that although Mongo’s wind resource is modest, its temporal stability makes it viable for decentralized applications. In a country like Chad – where rural electrification remains below 12% and energy access relies primarily on diesel generators and biomass<sup>3,4,5,30</sup> – the use of small wind systems could help reduce environmental degradation, particularly deforestation and indoor air pollution, while contributing to national climate commitments.<sup>42,43</sup>

Moreover, combining wind power with solar energy, which is abundant across the Sahel, can increase energy



**Figure 4. Wind power density in Mongo. (A) Annual averages from 2012 to 2022; (B) Monthly variations highlighting seasonal energy potential.**

**Table 4. Annual and monthly wind direction (°) for Mongo (2012 – 2022)**

Month	2012	2013	2014	2015	2016	2017	2018	2019	2020	2021	2022	Mean
Jan	38.25	34.81	28.19	34.06	33.00	49.44	45.44	18.69	52.5	51.31	17.88	36.69
Feb	59.19	41.94	37.19	26.00	40.94	41.56	32.00	15.81	35.12	33.38	30.12	35.75
Mar	46.75	61.25	40.19	58.25	38.44	30.88	56.44	54.12	46.44	65.12	55.44	50.30
Apr	124.50	86.00	180.62	56.69	104.81	121.25	89.25	83.75	98.12	83.88	196.19	111.37
May	184.75	197.19	187.06	171.00	184.50	185.31	204.62	212.12	201.00	158.00	214.25	190.89
Jun	219.25	204.06	195.56	213.44	200.06	210.75	191.94	196.38	205.75	195.44	199.44	202.92
Jul	223.38	206.75	213.31	202.94	215.38	216.25	205.62	202.44	209.75	208.38	219.62	211.26
Aug	224.94	228.56	215.00	211.06	210.81	231.75	220.00	216.12	227.88	193.38	230.25	219.07
Sept	221.62	236.75	187.38	206.31	197.56	196.88	180.44	178.12	201.06	183.38	199.75	199.02
Oct	196.12	150.69	144.62	196.06	127.5	120.62	123.88	124.19	70.19	93.50	98.31	131.43
Nov	69.62	50.44	105.44	53.19	95.12	70.12	96.81	92.88	57.31	80.44	55.31	75.15
Dec	40.50	47.19	51.19	35.94	65.19	48.31	42.19	58.50	70.69	49.56	58.56	51.62
Mean	137.41	128.80	132.15	122.08	126.11	126.93	124.05	121.09	122.98	116.31	131.26	126.29

**Table 5. Monthly and annual mean temperatures (°C) recorded in Mongo (2012 – 2022)**

Month	2012	2013	2014	2015	2016	2017	2018	2019	2020	2021	2022	Mean
Jan	25.00	26.69	25.33	22.83	23.61	27.30	22.69	26.85	22.47	25.47	24.70	24.81
Feb	29.18	29.15	27.76	28.94	26.82	27.38	29.48	28.33	26.48	26.49	25.96	27.82
Mar	30.05	31.58	31.65	31.63	33.19	30.88	31.31	31.90	31.46	31.84	30.97	31.50
Apr	33.37	32.53	33.04	31.66	33.98	33.81	32.89	33.70	33.80	32.73	33.60	33.19
May	31.18	32.55	31.80	33.86	33.59	33.75	31.98	33.43	32.96	32.65	31.36	32.65
Jun	27.78	29.99	30.56	30.58	29.43	29.15	29.44	29.32	30.09	29.88	28.50	29.52
Jul	25.30	26.88	26.98	27.61	26.14	27.01	26.61	27.35	27.22	26.66	26.44	26.75
Aug	24.45	24.40	24.64	25.33	25.06	25.52	24.98	24.79	24.85	25.40	24.48	24.90
Sep	25.05	25.33	25.19	25.55	25.85	25.97	25.49	25.79	25.03	25.30	25.11	25.42
Oct	25.98	26.53	25.80	26.78	26.60	27.77	26.09	25.01	25.41	26.64	25.51	26.19
Nov	26.01	27.12	25.64	25.92	27.20	27.83	26.30	24.04	24.00	25.73	24.13	25.81
Dec	23.94	25.21	24.74	22.44	25.87	26.42	25.64	22.02	25.14	25.65	23.01	24.55
Mean	27.27	28.16	27.76	27.76	28.11	28.57	27.74	27.71	27.41	27.87	26.98	27.76

reliability for off-grid systems. Hybrid solutions have been shown to enhance energy access in rural settings

while supporting essential services, such as healthcare, education, and agriculture.<sup>38,44</sup> This aligns with the

### Statistical analysis of wind energy

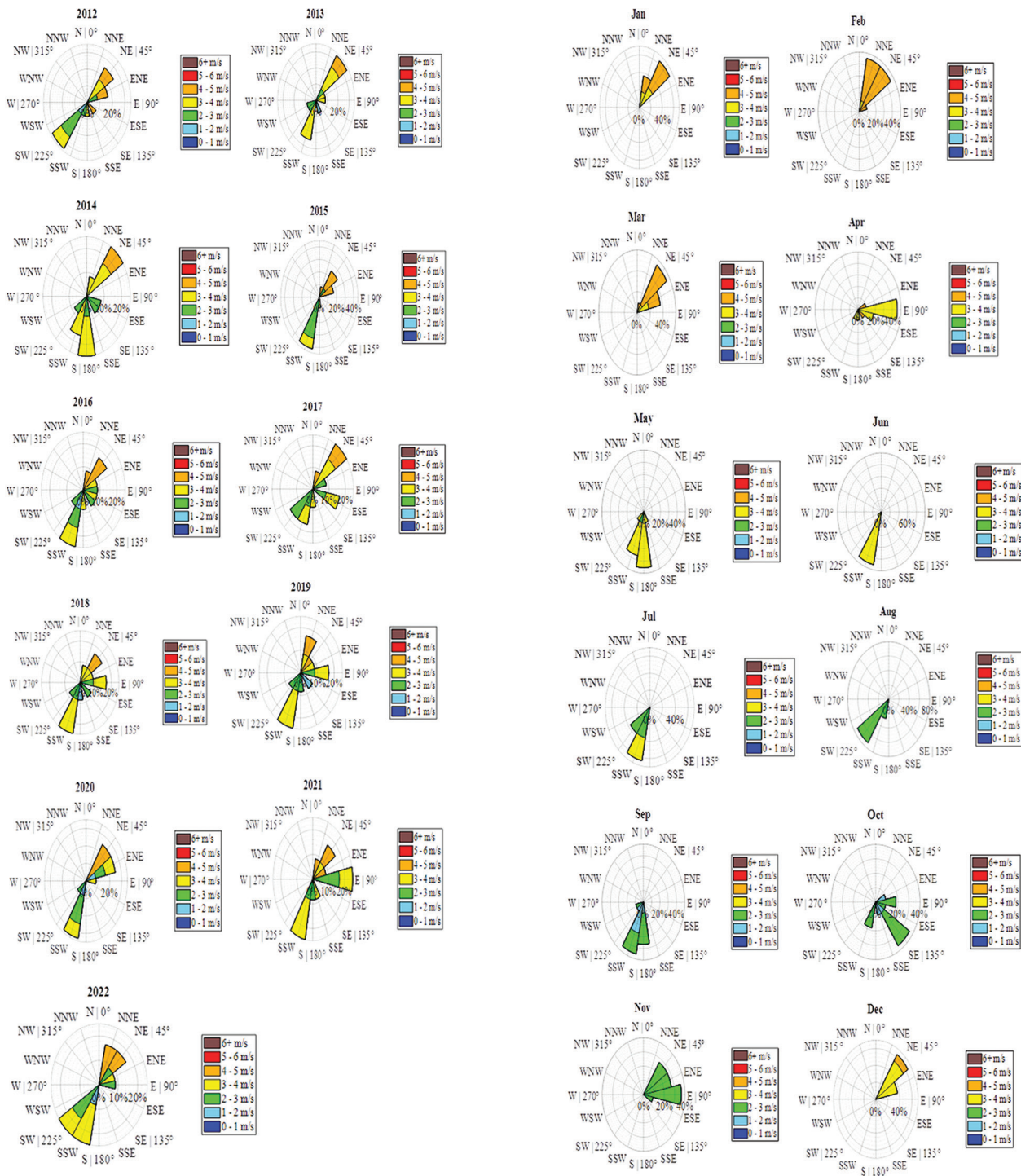


**Figure 5. Annual wind rose diagrams (2012 – 2022) for Mongo, depicting prevailing wind directions and interannual variability**

Abbreviations: E: East, ENE: East-northeast; ESE: East-southeast; N: North; NE: Northeast; NNE: North-northeast; NNW: North-northwest; NW: Northwest; S: South; SE: Southeast; SSE: South-southeast; SSW: South-southwest; SW: Southwest; W: West; WNW: West-northwest; WSW: West-southwest.

**Figure 6. Monthly wind rose diagrams showing seasonal changes in wind directions influencing turbine siting strategies**

Abbreviations: E: East, ENE: East-northeast; ESE: East-southeast; N: North; NE: Northeast; NNE: North-northeast; NNW: North-northwest; NW: Northwest; S: South; SE: Southeast; SSE: South-southeast; SSW: South-southwest; SW: Southwest; W: West; WNW: West-northwest; WSW: West-southwest.

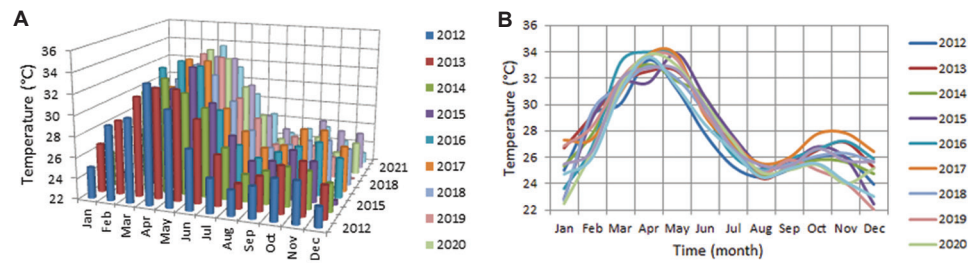


**Figure 7. Temperature profiles in Mongo (2012 – 2022). (A) 3D view of monthly temperature evolution; (B) 2D projection illustrating seasonal temperature cycles.**

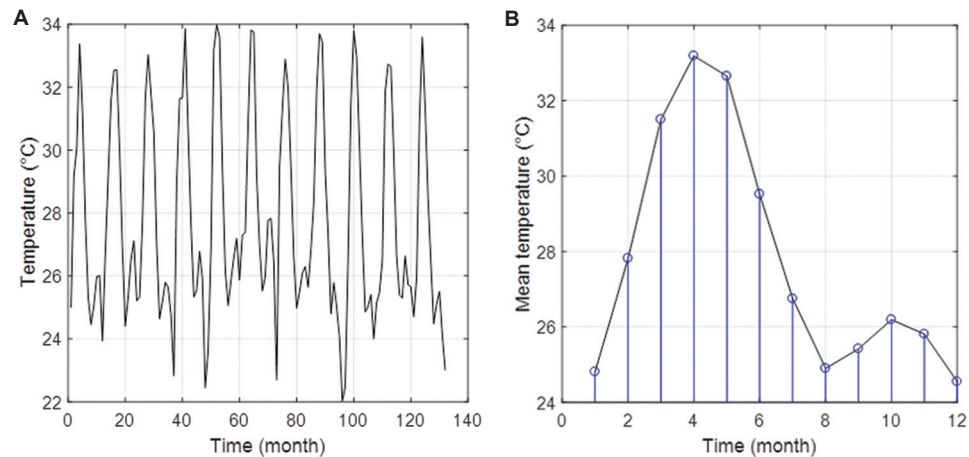


**Figure 8. Temporal temperature signals. (A) Raw monthly data; (B) Long-term average illustrating quasi-periodic burst patterns.**

Sustainable Development Goals (SDG 7: Affordable and clean energy, and SDG 13: Climate action).<sup>45</sup>

The observed seasonal and directional variations also underline the importance of adapting turbine technology and layout to local wind regimes. Appropriate turbine orientation can maximize efficiency and extend its lifespan.<sup>2,10,21,46</sup> In similar climatic contexts, locally optimized systems have demonstrated better environmental integration and operational stability.<sup>12,18,35</sup>

Overall, wind energy in regions, such as Mongo should not be neglected due to low average speeds. Instead, it should be considered a strategic component of a diversified, low-carbon energy mix that supports inclusive development and environmental sustainability.<sup>7,30,47,48</sup>

#### 4. Conclusion

This study presented a comprehensive statistical analysis of Mongo's wind energy potential over 11 years, applying the Weibull distribution to characterize wind speed patterns. The average annual wind speed of 3.2 m/s places Mongo in wind power Class 1, indicating a low-to-moderate wind resource suitable mainly for

small-scale and decentralized wind energy applications. The wind direction analysis reported predominant south-southwest winds with notable temporal and seasonal variability, emphasizing the importance of adaptive turbine placement and orientation to maximize energy capture. In addition, the warm climate with an average temperature of 27.76°C, combined with the observed non-linear relationship between temperature and wind speed, reflects complex local atmospheric dynamics that affect wind availability.

While the study highlights Mongo's modest but stable wind resource, some limitations should be acknowledged. The reliance on monthly-averaged data may mask short-term fluctuations and finer temporal wind variations that are important in assessing turbine performance. Furthermore, the use of a single meteorological station limits spatial representativeness, and some data gaps were present. These constraints suggest the need for higher-resolution temporal data and more extensive spatial measurements to fully capture the variability of wind resource.

Looking ahead, future research should focus on site-specific turbine optimization considering the variability

in wind direction and speed. Integrating wind energy with complementary renewable sources, such as solar power, could enhance energy reliability and supply for rural electrification. Moreover, economic feasibility studies and detailed spatial resource mapping will be crucial for designing effective, sustainable wind energy systems in Mongo and other similar regions.

## Acknowledgments

None.

## Funding

None.

## Conflict of interest

The authors declare that they have no competing interests.

## Author contributions

*Conceptualization:* Ali Sidick Bahar, Adoum Kriga, Ali Ramadan Ali

*Data curation:* Adoum Kriga, Adoum Danao Adile

*Formal analysis:* Ali Ramadan Ali, Fabien Kenmogne

*Methodology:* Ali Sidick Bahar, Adoum Kriga

*Writing – original draft:* Fabien Kenmogne

*Writing – review & editing:* All authors

## Availability of data

All data generated or analyzed during this study are included in this published article.

## References

- Nediguina MK, Tahir AM, Barka M, Soulouknga MH, Nsouandele JL. Evaluation of the wind power potential in the northeast of Chad. *J Renew Energies*. 2022;25(1):109-126. doi: 10.54966/jreen.v25i1.1075
- Soulouknga MH, Oyedepo SO, Doka SY, Kofané TC. Assessment of wind energy potential in the Sudanese zone in Chad. *Energy Power Eng*. 2017;9(7):386-402. doi: 10.4236/epe.2017.97026
- Ouedraogo AO, Doka SY, Revanna N, Djongyang N, Kofané TC. Analysis of wind speed data and wind energy potential in faya-largeau, chad, using weibull distribution. *Renew Energy*. 2018;121:1-8. doi: 10.1016/j.renene.2018.01.002
- International Energy Agency. *Africa Energy Outlook 2022*. Paris, France: IEA; 2022.
- Agence Pour Le Développement Des Energies Renouvelables (ADER) Et Ministère Du Pétrole Et De l'Énergie Du Tchad. *Plan Général D'action Des Energies Renouvelables 2017-2030*. N'Djaména, Tchad: ADER; 2017.
- Tchinda R, Kendjio J, Kaptoum E, Njomo D. Estimation of mean wind energy available in far north Cameroon. *Energy Convers Manage*. 2000;41(17):1917-1929. doi: 10.1016/S0196-8904(00)00017-0
- United Nations Environment Programme. *Renewable Energy Law and Policy Review: Selected African Countries*. Nairobi, Kenya: UNEP; 2019.
- Kassem Y, Çamur H, Abughinda SAM, Şefik A. Wind energy potential assessment in selected regions in northern cyprus based on weibull distribution function. *J Eng Appl Sci*. 2020;15(1):128-140. doi: 10.3923/jeasci.2020.128.140
- Akpınar EK, Akpınar S. A statistical analysis of wind speed data used in installation of wind energy conversion systems. *Energy Convers Manage*. 2005;46(4):515-532. doi: 10.1016/j.enconman.2004.07.007
- Ahmed Shata AS, Hanitsch R. Evaluation of wind energy potential and electricity generation on the coast of Mediterranean Sea in Egypt. *Renew Energy*. 2006;31:1183-1202. doi: 10.1016/j.renene.2005.07.012
- Celik AN. Statistical analysis of wind power density based on the Weibull and Rayleigh models at the southern region of Turkey. *Renew Energy*. 2004;29:593-604. doi: 10.1016/j.renene.2003.07.001
- Carta JA, Ramirez P, Velazquez S. A review of wind speed probability distributions used in wind energy analysis: Case studies in the Canary Islands. *Renew Sustain Energy Rev*. 2009;13(5):933-955. doi: 10.1016/j.rser.2008.02.008
- Zhou J, Erdem E, Li G, Shi J. Comprehensive evaluation of wind speed distribution models: A case study for North Dakota sites. *Energy Convers Manage*. 2010;51:1449-1458. doi: 10.1016/j.enconman.2010.01.005
- Chellali F, Khellaf A, Belouchrani A, Khanniche R. A comparison between wind speed distributions derived from the maximum entropy principle and Weibull distribution. Case of study; six regions of Algeria. *Renew Sustain Energy Rev*. 2012;16(1):379-385. doi: 10.1016/j.rser.2011.08.002
- Li M, Li X. Investigation of wind characteristics and assessment of wind energy potential for Waterloo Region, Canada. *Energy Convers Manage*. 2005;46:3014-3033. doi: 10.1016/j.enconman.2005.02.011
- Okorie OC, Ajayi NO, Bamisile OS, et al. Evaluating wind energy resources for remote communities in West

- Africa. *Renew Sustain Energy Rev.* 2022;160:112282.  
doi: 10.1016/j.rser.2022.112282
17. Ghasemi A, Hosseini AS, Marashi SPH. Wind energy resource assessment using Weibull parameters and GIS: A case study for the province of Yazd. *Renew Sustain Energy Rev.* 2013;28:496-504.  
doi: 10.1016/j.rser.2013.08.016
  18. Ghaffari M, Alavi A, Dehghan S. Wind energy potential assessment in arid regions using GIS-based Weibull analysis: A case study in central Iran. *Renew Energy.* 2021;168:1241-1252.  
doi: 10.1016/j.renene.2021.01.115
  19. Gupta NK, Kumar S. Statistical modeling of wind speed and wind power assessment using Weibull and Rayleigh models in India. *Energy Rep.* 2020;6:2431-2441.  
doi: 10.1016/j.egy.2020.08.099
  20. Kim TH, Lim HC. A comparative study of wind speed distributions using entropy and Weibull functions. *Energies.* 2020;13(4):1-18.  
doi: 10.3390/en13040954
  21. Nyarko KA, Whale J, Urmee T. Drivers and challenges of off-grid renewable energy-based projects in West Africa: A review. *Heliyon.* 2023;9(5):e16710.  
doi: 10.1016/j.heliyon.2023.e16710
  22. Nasiri F, Yari M, Ameri M. Wind resource assessment and feasibility study in southeastern Iran. *Renew Energy.* 2021;164:869-882.  
doi: 10.1016/j.renene.2020.08.037
  23. Nasiri AA, Yılmaz A, Özdemir E. Assessment of wind energy potential using Weibull parameters: A case study from Turkey. *Energy Sources A.* 2023;45(6):1154-1170.  
doi: 10.1080/15567036.2020.1751015
  24. Medjo Nouadje BA, Kelly E, Djiela RHT, Kapen PT, Tchuen G, Tchinda R. Chad's wind energy potential: An assessment of Weibull parameters using thirteen numerical methods for a sustainable development. *Int J Ambient Energy.* 2023;45(1):2276119.  
doi: 10.1080/01430750.2023.2276119
  25. Aslam M, Raza SAR, Khan TH. Wind energy assessment for remote areas in Pakistan. *Energy Rep.* 2020;6:1547-1558.  
doi: 10.1016/j.egy.2020.02.017
  26. Gökçek M, Bayülgen M. A feasibility study for wind energy in Kırklareli, Turkey. *Renew Sustain Energy Rev.* 2007;11(9):2183-2190.  
doi: 10.1016/j.rser.2006.04.012
  27. Petkovic D, Ilic D, Milinkovic M. Comparison of wind speed models for low wind resource sites. *Energy.* 2020;210:118572.  
doi: 10.1016/j.energy.2020.118572
  28. Saidur R, Rahim NA, Islam MR, Solangi KH. A review on global wind energy policy. *Renew Sustain Energy Rev.* 2010;14:1744-1762.  
doi: 10.1016/j.rser.2010.03.008
  29. Yu X, Qu H. Wind power in China-opportunity goes with challenge. *Renew Sustain Energy Rev.* 2010;14:2232-2237.  
doi: 10.1016/j.rser.2009.11.003
  30. International Renewable Energy Agency. *Off-Grid Renewable Energy Systems: Status and Methodological Issues.* Abu Dhabi, UAE: IRENA; 2015.
  31. Arreyndip NA, Joseph E. Generalized extreme value distribution models for the assessment of seasonal wind energy potential of Debuncha, Cameroon. *J Renew Energy.* 2016;2016:9357812.  
doi: 10.1155/2016/9357812
  32. Tuncar EA, Sağlam S, Oral B. A review of short-term wind power generation forecasting methods in recent technological trends. *Energy Rep.* 2024;12:197-209.  
doi: 10.1016/j.egy.2024.06.006
  33. Jeon J, Taylor JW. Using conditional kernel density estimation for wind power density forecasting. *J Am Stat Assoc.* 2012;107(497):66-79.  
doi: 10.1080/01621459.2011.643745
  34. Jurado X, Reiminger N, Vazquez J, Wemmert C. On the minimal wind directions required to assess mean annual air pollution concentration based on CFD results. *Sustain Cities Soc.* 2021;71:102920.  
doi: 10.1016/j.scs.2021.102920
  35. Mandal S, Kundu S, Mondal S. Statistical modeling of wind speed data using empirical and theoretical distributions. *Renew Energy,* 2019;134:983-992.  
doi: 10.1016/j.renene.2018.11.056
  36. Jeutho MG, Kenmogne F, Yemélé D. How to use the temperature data to find the appropriate site for best wind speed generation? Applications on data obtained from three different cities of Cameroon. *Int J Sci Eng Sci.* 2018;2(4):53-62.
  37. Grace EA, Rekha ASP, Thenaras M. Automated solar powered pumping systems for irrigation. *Int J Pure Appl Math.* 2017;114(7):507-516.
  38. Mostafaeipour A, Jadidi M, Mohammadi K, Sedaghat A. An analysis of wind energy potential and economic evaluation in Zahedan, Iran. *Renew Sustain Energy Rev.* 2014;30:641-650.  
doi: 10.1016/j.rser.2013.11.016
  39. Ali RA, Nediguina MK, Gouajio M, et al. Effects of adding the antiparallel diodes in a model of solar photovoltaic cell: Theory and PSpice simulations. *J Mod Green Energy.* 2024;3:4.  
doi: 10.53964/jmge.2024004
  40. Jeutho MG, Kenmogne F, Yemélé D. Statistical estimation of mean wind energy available in western region of Cameroon: Case of the Bafoussam's city. *J Harmoniz Res Eng.* 2017;5(1):15-27.
  41. Manwell JF, McGowan JG, Rogers AL. *Wind Energy Explained: Theory, Design and Application.* 2<sup>nd</sup>ed. Chichester, UK: Wiley; 2009.
  42. Ouedraogo NS. Modeling sustainable long-term electricity supply-demand in Africa. *Appl Energy.*

- 2017;190:1047-1067.  
doi: 10.1016/j.apenergy.2016.12.162
43. Bishoge OK, Kombe GG, Mvile BN. Renewable energy for sustainable development in Sub-Saharan African countries: Challenges and way forward. *J Renew Sustain Energy*. 2020;12(5):052702.  
doi: 10.1063/5.0009297
44. Bhandari B, Lee KT, Lee CS, Song CK, Maskey RK, Ahn SH. A review on solar and wind energy systems for off-grid rural electrification in developing countries. *Renew Sustain Energy Rev*. 2014;38:258-268.  
doi: 10.1016/j.rser.2014.05.057
45. United Nations. *Transforming our World: The 2030 Agenda for Sustainable Development*. UN Res A/RES/70/1. New York, NY: United Nations; 2015.
46. Bekele G, Palm B. Feasibility study for a standalone solar-wind-based hybrid energy system for application in Ethiopia. *Appl Energy*. 2010;87(2):487-495.  
doi: 10.1016/j.apenergy.2009.06.006
47. Abdmouleh Z, Alammari RAM, Gastli A. Recommendations on renewable energy policies for the GCC countries. *Renew Sustain Energy Rev*. 2015;50:1181-1191.  
doi: 10.1016/j.rser.2015.05.057
48. Hadjipaschalis I, Poullikkas A, Efthimiou V. Overview of current and future energy storage technologies for electric power applications. *Renew Sustain Energy Rev*. 2009;13(6-7):1513-1522.  
doi: 10.1016/j.rser.2009.06.045